Layer- and Bulk-Roton Excitations of ^{4}He in Porous Media

V. Apaja and E. Krotscheck

Institut für Theoretische Physik, Johannes Kepler Universität, A 4040 Linz, Austria

(Received 18 May 2003; published 26 November 2003)

We examine the energetics of bulk- and layer-roton excitations of ^{4}He in various porous medial such as aerogel, Geltech, or Vycor, in order to find out what conclusions can be drawn from experiments on the energetics about the physisorption mechanism. The energy of the layer-roton minimum depends sensitively on the substrate strength, thus providing a mechanism for a direct measurement of this quantity. On the other hand, bulklike roton excitations are largely independent of the interaction between the medium and the helium atoms, but the dependence of their energy on the degree of filling reflects the internal structure of the matrix and can reveal features of ^{4}He at negative pressures. While bulklike rotons are very similar to their true bulk counterparts, the layer modes are not in close relation to two-dimensional rotons and should be regarded as a third, completely independent kind of excitation.

DOI: 10.1103/PhysRevLett.91.225302 PACS numbers: 67.70.+n

Collective excitations of superfluid helium confined in various porous media have been studied by neutron scattering since the early 1990's, and by now a wealth of information about helium in aerogel, Vycor, and Geltech has been collected [1–10]. Aerogel is an open gel structure formed by silica strands (SiO_2). Typical pore sizes range from a few Å to a few hundred Å, without any characteristic pore size. Vycor is a porous glass, where pores form channels of about 70 Å diameter. Geltech resembles aerogel, except that the nominal pore size is 25 Å [9].

Liquid ^{4}He is adsorbed in these matrices in the form of atomic layers; the first layer is expected to be solid. On a more strongly binding substrate, such as graphite, one expects two solid layers. Energies and lifetimes of phonon-roton excitations for confined ^{4}He are nearly equal to their bulk superfluid ^{4}He values for filled cells [11], but differences become observable at partial fillings when the bulk signal is weaker. The appearance of ripplons is tied to the existence of a free liquid surface; neutron scattering experiments show clearly their presence in adsorbed films [10,12,13] with few layers of helium.

An exclusive feature of adsorbed films is the appearance of "layer modes." The existence of such excitations has been proposed in the 1970's [14,15] from theoretical calculations of the excitations of two-dimensional ^{4}He and comparison with specific heat data. Direct experimental evidence for the existence of collective excitations below the roton minimum has first been presented by Lauter and collaborators [13,16]. Identification of these excitations with longitudinally polarized phonons that propagate in the liquid layer adjacent to the substrate has been provided by microscopic calculations of the excitations of films [17,18].

In an experimental situation, the topology gives rise to a nonuniform filling of the pores. But from the theoretical point of view different materials are characterized solely by their substrate potentials, because as long as the wavelength of the excitation in concern is much shorter than any porosity length scale, the topology of the confining matrix is immaterial. We therefore examine the energetics of the layer roton as a function of the substrate-potential strength which determines, in turn, the areal density in the first liquid layer, obtained by integrating the density up to the first minimum. For that purpose, we have carried out a number of calculations of the structure of helium films as a function of potential strength. The microscopic theory behind these calculations is described in Ref. [19]. Our model assumes the usual 3-9 potential

$$U_3(z) = \left[\frac{4C_3^3}{27D^2}\right]\frac{1}{z^9} - \frac{C_3}{z^3}; \qquad (1)$$

we have varied the potential strength D from 8 to 50 K and the range C_3 from 1000 to 2500 K Å^3. In all cases, we have considered rather thick films of an areal density of 0.45 Å^{-2}. Figure 1 shows density profiles for these potential strengths close to the substrate; the density profiles are practically independent of the potential range C_3.

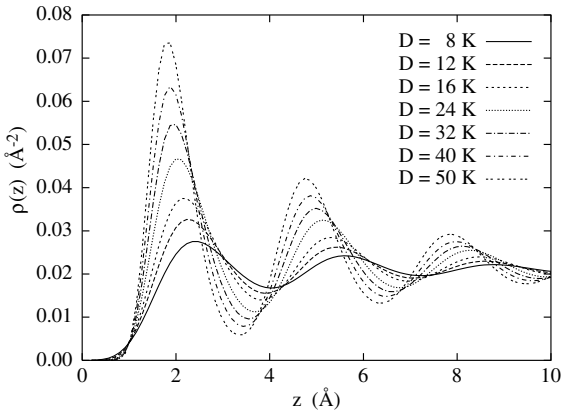

FIG. 1. The density profiles of the first three layers are shown as a function of the depth D of the substrate potential. The substrate is at $z < 0$.

To introduce excitations to the system one applies a small, time-dependent perturbation that momentarily drives the quantum liquid out of its ground state. Generalizing the Feynman-Cohen wave function [20], we write the excited state in the form

$$|\Psi(t)\rangle = \frac{e^{-iE_0 t/\hbar}\, e^{1/2\delta U(t)}|\Psi_0\rangle}{[\langle\Psi_0|e^{\mathrm{Re}\delta U(t)}|\Psi_0\rangle]^{1/2}}, \quad (2)$$

where $|\Psi_0\rangle$ is the exact or an optimized variational ground state, and the excitation operator is

$$\delta U(t) = \sum_i \delta u_1(\mathbf{r}_i; t) + \sum_{i<j} \delta u_2(\mathbf{r}_i, \mathbf{r}_j; t) + \cdots . \quad (3)$$

The time-dependent excitation functions $\delta u_n(\mathbf{r}_1, \ldots, \mathbf{r}_n; t)$ are determined by an action principle

$$\delta \int_{t_0}^{t_1} dt \left\langle \Psi(t) \left| H - i\hbar\frac{\partial}{\partial t} + U_{\mathrm{ext}}(t) \right| \Psi(t) \right\rangle = 0, \quad (4)$$

where $U_{\mathrm{ext}}(t)$ is the weak external potential driving the excitations. The truncation of the sequence of fluctuating correlations δu_n in Eq. (3) defines the level of approximation in which we treat the excitations. One recovers the Feynman theory of excitations [21] for nonuniform systems [22] by setting $\delta u_n(\mathbf{r}_1, \ldots, \mathbf{r}_n; t) = 0$ for $n \geq 2$. The two-body term $\delta u_2(\mathbf{r}_1, \mathbf{r}_2; t)$ describes the time dependence of the short-ranged correlations. It is plausible that this term is relevant when the wavelength of an excitation becomes comparable to the interparticle distance. Consequently, the excitation spectrum can be quite well understood [23–25] by retaining only the time-dependent one- and two-body terms in the excitation operator (3). The simplest nontrivial implementation of the theory leads to a density-density response function of the form [17]

$$\chi(\mathbf{r}, \mathbf{r}', \omega) = \sqrt{\rho(\mathbf{r})}\sum_{st} \phi^{(s)}(\mathbf{r})[G_{st}(\omega) + G_{st}(-\omega)]\phi^{(t)}(\mathbf{r}')\sqrt{\rho(\mathbf{r}')}, \quad (5)$$

where the $\phi^{(s)}(\mathbf{r})$ are Feynman excitation functions, and

$$G_{st}(\omega) = [\hbar[\omega - \omega_s + i\epsilon]\delta_{st} + \Sigma_{st}(\omega)]^{-1}, \quad (6)$$

the phonon propagator. The fluctuating pair correlations give rise to the dynamic self-energy correction [17],

$$\Sigma_{st}(\omega) = \frac{1}{2}\sum_{mn} \frac{V_{mn}^{(s)} V_{mn}^{(t)}}{\hbar(\omega_m + \omega_n - \omega)}. \quad (7)$$

Here, the summation is over the Feynman states m, n; they form a partly discrete, partly continuous set due to the inhomogeneity of the liquid. The expression for the three-phonon coupling amplitudes $V_{mn}^{(s)}$ can be found in Ref. [17]. This self-energy renormalizes the Feynman "phonon" energies $\hbar\omega_n$ and adds a finite lifetime to states that can decay. The form of the self-energy given in Eq. (7) is the generalization of the correlated basis functions (CBF) [23,24] theory to inhomogeneous systems. As a final refinement of the theory, we scale the Feynman energies ω_n appearing in the energy denominator of the self-energy given in Eq. (7) such that the roton minimum of the spectrum used in the energy denominator of Eq. (7) agrees roughly with the roton minimum predicted by the calculated $S(\mathbf{k}, \omega)$. This is a computationally simple way of adding the self-energy correction to the excitation energies in the denominator of Eq. (7). We shall use this approximation for the numerical parts of this paper. In the case of ^{4}He film on graphite the present theory gives excitation spectra, which are in very good agreement with neutron scattering results [16].

Layer phonons appear in the dynamic structure function $S(\mathbf{k}, \omega)$ as peaks below the roton minimum. A gray scale map of a typical dynamic structure function is shown in Fig. 2; we have for clarity chosen a momentum transfer parallel to the substrate. Neutron scattering at other angles would show a different layer-roton dispersion, because the in-plane momentum transfer varies with angle [18]. The figure shows in fact one bulk- and two layer-roton minima, but the higher one, which corresponds to an excitation propagating in the second liquid layer, has an energy too close to the bulk roton to be experimentally distinguishable.

The time-dependent part of the total density is the transition density, defined as $\delta\rho(\mathbf{r}, t) = \langle\Psi_0|\hat{\rho}(\mathbf{r})|\Psi(t)\rangle - \langle\Psi_0|\hat{\rho}(\mathbf{r})|\Psi_0\rangle$ + c.c. In momentum space the transition densities are the probability amplitudes which, together with the excitation energies, are all that one needs to construct the dynamic structure function. In coordinate space they also tell us where the density changes related to some specific excitation reside. The transition densities corresponding to the three pronounced excitations at $k = 1.8$ Å^{-1} are depicted in Fig. 3. The figure shows that the

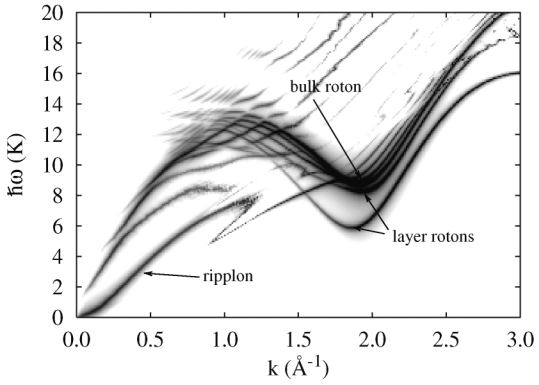

FIG. 2. The figure shows the map of the dynamic structure function $S(\mathbf{k}, \omega)$ for a ^{4}He film for the potential strength $D = 24$ K. The two layer rotons, the bulk roton, and the ripplon are indicated by arrows. Notice how the lower energy layer roton has minimum at lowest k, meaning it experiences the highest "effective" density. Indeed, the corresponding transition density depicted in Fig. 3 has nodes at the density minima.

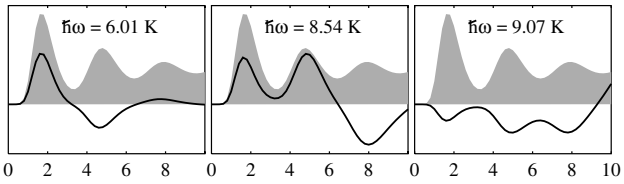

FIG. 3. The transition densities of the three lowest excitations are shown as a function of z (in Å) for $D = 24$ K and $C_3 = 1500$ K Å^3, normalized to the same maximum value. For comparison, the density profile of the film is shown as a gray-shaded area.

two layer modes are located in the first two layers adjacent to the substrate, whereas the "bulk" mode is spread throughout the liquid. Clearly, the notion that the wave propagates in the first or the second layer is also not quite accurate: The lowest mode also has some overlap with the second layer, but especially the second mode spreads over both layers.

We have carried out two independent calculations of the roton excitation: First, we calculated the roton energy as a function of the density for a rigorously two-dimensional liquid. We can assess the accuracy of our predictions with the shadow-wave-function calculation of $S(\mathbf{k}, \omega)$ of Ref. [26], which obtained a roton energy of 5.67 ± 0.2 K at the equilibrium density of $n = 0.0421$ Å^{-2}. Second, we have calculated the dynamic structure function $S(\mathbf{k}, \omega)$ in the relevant momentum region for the above family of substrate potentials. The results are compiled in Fig. 4 where we also collect several experimental values.

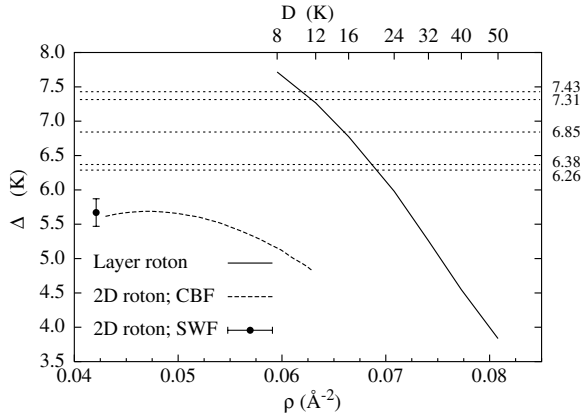

FIG. 4. The figure shows the energy of the 2D roton (long-dashed line) and the energy of the layer roton in a film (solid line) as a function of areal density. The upper horizontal axis shows the corresponding values of the well depth D. Also shown is the energy of a two-dimensional roton obtained with shadow wave functions (SWF) [26]. The short-dashed horizontal lines show experimental values of the layer-roton energy on aerogel [6,10] (7.31 and 7.43 K), Geltech [9] (6.85 K), Vycor [7,8] (6.38 K), and graphite [27] (6.26 K). Their energies are marked in the right margin.

Although exactly the same method has been used for the computation of the purely 2D system and for the films, the results are quite different. We have obtained for the film calculation a layer density by integrating the three-dimensional densities shown in Fig. 1 to the first minimum. This is evidently not very well defined for the weakly bound systems, but it is not legitimate either for the case of strong binding where the first layer is well defined. In fact, the integrated density for the strongest substrate is 0.08 Å^{-2}, which is well beyond the solidification density of the purely two-dimensional system. Evidently, the zero-point motion in the z direction can effectively suppress the phase transition. We make therefore three conclusions: (i) The position of the layer-roton minimum is indeed a sensitive measure for the strength of the substrate potential, (ii) purely two-dimensional models are manifestly inadequate for their understanding, and, hence, (iii) purely two-dimensional models are also questionable for interpreting thermodynamic data of adsorbed films.

With few exceptions, the bulk-roton energy in porous media has been reported to be practically identical to that in the bulk liquid. Reference [6] reports a slight increase of the roton energy in aerogel at partial filling. A roton energy above the bulk one can be explained by assuming that the density of the helium liquid seen by the excitation is below that of the bulk liquid. In the case of helium filling a confined space a lower density in the middle of the space can be qualitatively explained by the cost in energy to form a surface. In the case of partial filling (films) there is the low-density surface region that decreases the "effective" density. There is a reason to believe that this also decreases the maxon energy, observed by Lauter *et al.* [12] in thin films on graphite.

To be quantitative, we have performed calculations of the energetics and structure of ^{4}He in a gap between attractive silica walls [18] and obtained the energy of the bulk roton (cf. Fig. 2) as a function of filling. Figure 5 shows, as a typical example, the roton energetics in a gap of 25 Å width. The independent parameter is the areal density n; the corresponding three-dimensional density was obtained by averaging the density profile over the full volume. It is seen that the equilibrium density is well below the bulk value. In other words, the roton energy in a confined liquid should correspond to the one of a liquid that would, without confinement, have a negative pressure. The energy increase of the roton minimum found in this model is about 0.5 K, which is consistent with the experiments of Ref. [6].

To verify this interpretation of the data, it would be very useful to have comparable measurements for porous media with a more uniform distribution of pore sizes. In particular, comparably small pores should allow densities that are even below the bulk spinodal density [28], thus facilitating experiments on ^{4}He in density areas that were up to now inaccessible.

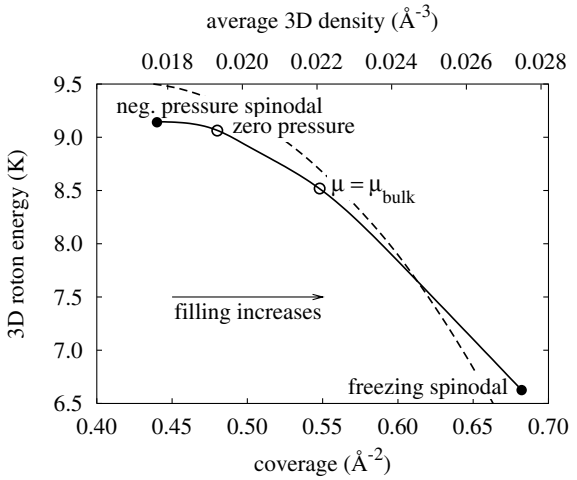

FIG. 5. The figure shows the energy of the bulk roton in a gap of 25 Å width as a function of the two-dimensional coverage and the corresponding average density. The points of zero pressure, the low-density and the high-density spinodal points, and the bulk chemical potential are indicated as points. The dashed line shows the roton energy of a purely 3D calculation.

We have shown that in confined liquid helium the bulk rotons are very similar to their true 3D bulk counterparts. In contrast to this, the layer modes are not confined to a single layer and bear no close relationship with strictly 2D rotons. The density range is different due to the compression of the liquid by the substrate potential. The layer-roton energies can be as high as about 8 K in low-coverage cases, while two-dimensional rotons never seems to reach 6 K. The experimental data on aerogel, Vycor, and Geltech are interpreted to show that layer rotons in porous media are actually halfway between two- and three-dimensional excitations and we argue that layer rotons should be regarded as a third, completely independent kind of excitation.

The energy of the low-energy layer mode is a sensitive measure of the potential well depth at the first liquid layer. The scan over different well depths and ranges of the potential shows that the latter plays no role for layer modes. The range of well depths at the first liquid layer is limited by solidification and dewetting.

This work was supported by the Austrian Science Fund (FWF) under Project No. P12832-TPH.

[1] P. E. Sokol, M. R. Gibbs, W. G. Stirling, R. T. Azuah, and M. A. Adams, Nature (London) **379**, 616 (1996).
[2] R. M. Dimeo, P. E. Sokol, D. W. Brown, C. R. Anderson, W. G. Stirling, M. A. Adams, S. H. Lee, C. Rutiser, and S. Komarneni, Phys. Rev. Lett. **79**, 5274 (1997).
[3] R. M. Dimeo, P. E. Sokol, C. R. Anderson, W. G. Stirling, and M. A. Adams, J. Low Temp. Phys. **113**, 369 (1998).
[4] M. R. Gibbs, P. E. S. W. G. Stirling, R. T. Azuah, and M. A. Adams, J. Low Temp. Phys. **107**, 33 (1997).
[5] H. R. Glyde, B. Fåk, and O. Plantevin, J. Low Temp. Phys. **113**, 537 (1998).
[6] B. Fåk, O. Plantevin, H. R. Glyde, and N. Mulders, Phys. Rev. Lett. **85**, 3886 (2000).
[7] H. R. Glyde, O. Plantevin, B. Fåk, G. Coddens, P. S. Danielson, and H. Schober, Phys. Rev. Lett. **84**, 2646 (2000).
[8] O. Plantevin, B. Fåk, H. R. Glyde, N. Mulders, J. Bossy, G. Coddens, and H. Schober, Phys. Rev. B **63**, 224508 (2001).
[9] O. Plantevin, H. R. Glyde, B. Fåk, J. Bossy, F. Albergamo, N. Mulders, and H. Schober, Phys. Rev. B **65**, 224505 (2002).
[10] H. J. Lauter, I. V. Bogoyavlenskii, A. V. Puchov, H. Godfrin, S. Skomorokhov, J. Klier, and P. Leiderer, Appl. Phys. (Suppl.) A **74**, S1547 (2002).
[11] C. R. Anderson, K. H. Andersen, J. Bossy, W. G. Stirling, R. M. Dimeo, P. E. Sokol, J. C. Cook, and D. W. Brown, Phys. Rev. B **59**, 13 588 (1999).
[12] H. J. Lauter, H. Godfrin, and P. Leiderer, J. Low Temp. Phys. **87**, 425 (1992).
[13] H. J. Lauter, H. Godfrin, V. L. P. Frank, and P. Leiderer, Phys. Rev. Lett. **68**, 2484 (1992).
[14] T. C. Padmore, Phys. Rev. Lett. **32**, 826 (1974).
[15] W. Götze and M. Lücke, J. Low Temp. Phys. **25**, 671 (1976).
[16] B. E. Clements, H. Godfrin, E. Krotscheck, H. J. Lauter, P. Leiderer, V. Passiouk, and C. J. Tymczak, Phys. Rev. B **53**, 12 242 (1996).
[17] B. E. Clements, E. Krotscheck, and C. J. Tymczak, Phys. Rev. B **53**, 12 253 (1996).
[18] V. Apaja and E. Krotscheck, Phys. Rev. B **67**, 184304 (2003).
[19] B. E. Clements, J. L. Epstein, E. Krotscheck, and M. Saarela, Phys. Rev. B **48**, 7450 (1993).
[20] R. P. Feynman and M. Cohen, Phys. Rev. **102**, 1189 (1956).
[21] R. P. Feynman, Phys. Rev. **94**, 262 (1954).
[22] C. C. Chang and M. Cohen, Phys. Rev. A **8**, 1930 (1973).
[23] H. W. Jackson, Phys. Rev. A **8**, 1529 (1973).
[24] C. C. Chang and C. E. Campbell, Phys. Rev. B **13**, 3779 (1976).
[25] V. Apaja and M. Saarela, Phys. Rev. B **57**, 5358 (1998).
[26] R. E. Grisenti and L. Reatto, J. Low Temp. Phys. **109**, 477 (1997).
[27] W. Thomlinson, J. A. Tarvin, and L. Passell, Phys. Rev. Lett. **44**, 266 (1980).
[28] V. Apaja and E. Krotscheck, J. Low Temp. Phys. **123**, 241 (2001).